Zuschriften

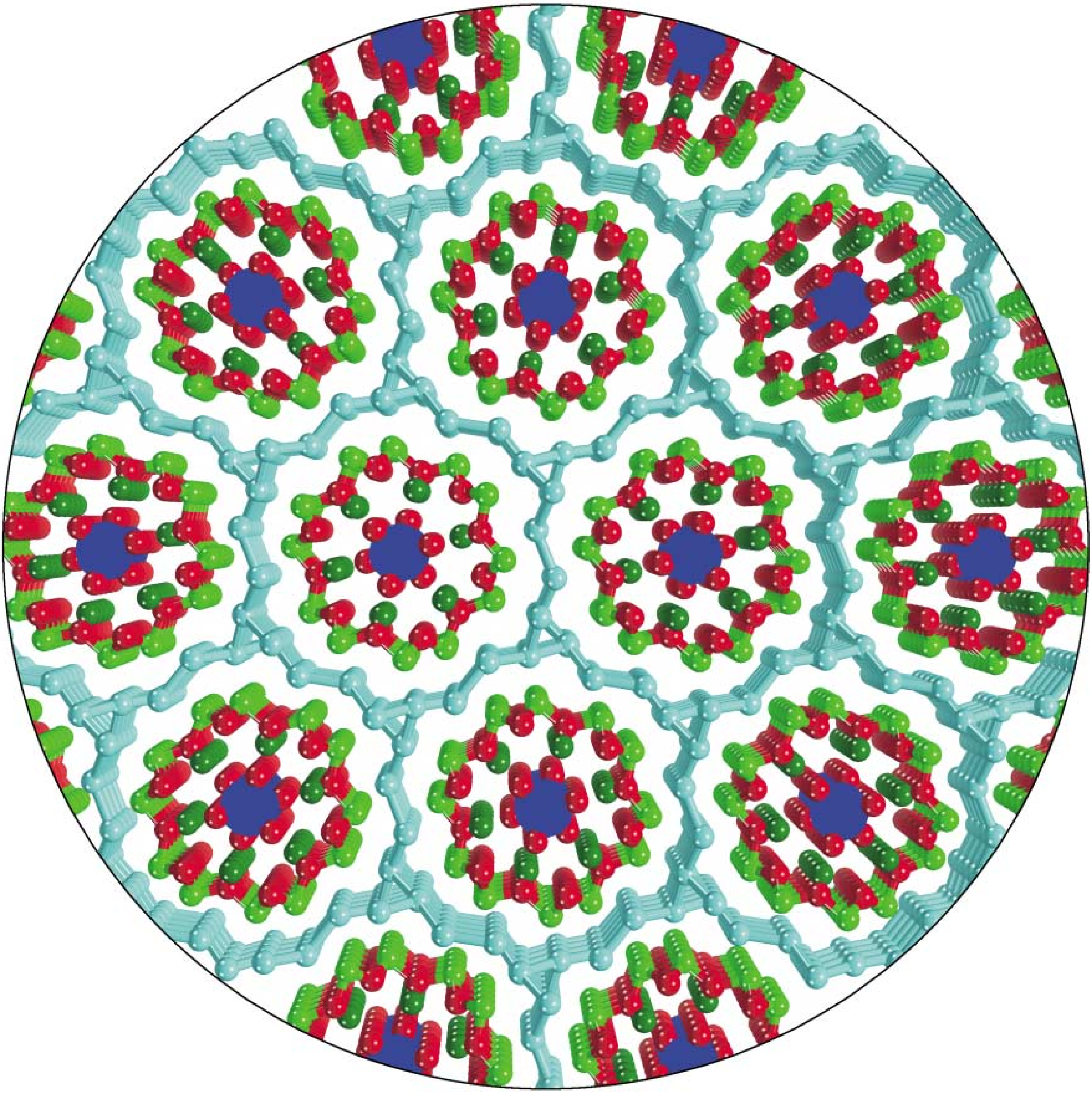

Ein kristalliner mikroporöser Halbleiter mit schmaler Bandlücke und hoher anisotroper Leitfähigkeit besteht aus einem Gerüst von Tellurkanälen, die ihrerseits kanalförmige Antimonoxid-Einheiten mit eingelagerten Kaliumionen und Wassermolekülen einschließen. Mehr dazu erfahren Sie in der Zuschrift von A. E. C. Palmqvist et al. auf den folgenden Seiten.

DOI: 10.1002/ange.200351284

Semiconductors

A Crystalline Microporous Narrow-Bandgap Semiconductor**

Anders E. C. Palmqvist, Bo B. Iversen,*
Ezio Zanghellini, Mårten Behm, and Galen D. Stucky

Crystalline microporous solids are of great importance and interest for many chemical and physical applications, due to their ordered arrangements of monodisperse channels, cavities, and cages in the molecular size regime where quantum effects occur. The best known group of these so-called molecular-sieve materials are the zeolites and zeolite-type metal oxides, which have applications in, for example, catalysis, adsorption, and ion-exchange processes. Zeolites are insulators due to their chemical composition, and although much effort have been made over the past 15 years to prepare semiconducting zeolite analogues, it was not until recently that an ordered 2 × 2 × 1 superstructure of the crystalline microporous mineral cetineite[2] with the composition $|K_3(H_2O)_3|[Sb_7O_9Se_3]$ was found to be a photo-semiconductor with a bandgap of 2.06 eV.[3] The optical bandgap of the cetineite-type phases was found to depend on the elemental composition and is, for example, 2.5 eV in $|Na_6(H_2O)_6|[Sb_{14}O_{18}S_6]$.[4]

Apparently, tellurium does not form the cetineite structure,[5] but we have found that by using a different synthesis approach, a new microporous semiconductor can be prepared.[6] The structure, referred to as SBC-1 (SBC = Santa Barbara–Chalmers), includes the potassium and water-containing $\{Sb_{12}O_{18}\}$ tubes found in cetineite but in addition SBC-1 has a unique tubular tellurium structural unit replacing the $\{SbSe_3\}$ pyramids present in cetineite, and a bandgap of merely 0.25 eV. This is a very narrow bandgap for microporous materials compared with, for example, 1.32 eV reported by Hanko and Kanatzidis for $RbCuSb_2Se_4{\cdot}H_2O$.[7] To our knowledge this is the first crystalline microporous antimony(III) oxide telluride. In addition, SBC-1 appears to be the first example of a second-order "zeoate" according to the definitions given in the most recent microporous materials nomenclature.[1] The new class of SBC-1 materials opens up a wide field of potential applications that are unique to the domain of microporous narrow-bandgap semiconductors.

Black SBC-1 needlelike crystals of a few millimeters in length and a diameter of approximately 0.1 mm were formed during the solvothermal treatment of a mixture of *n*-propylamine, aqueous KOH, Te, and Sb (trigonal space group $R\bar{3}$ (no. 148); hexagonal axes $a = b = 27.3361(11)$, $c = 5.6909(3)$ Å at 293 K). The crystal structure of SBC-1, as solved by single crystal XRD, is presented in Figure 1 with the hydrogen atoms in the water molecules (O_w) removed for clarity. The structure contains the characteristic 12-ring $\{Sb_{12}O_{18}\}$ tubular unit, with a ring width of 6.70 × 6.76 Å (assuming a van der Waals radius $r(O) = 1.35$ Å). The unit is built up from pyramidal $\{SbO_3\}$ groups linked together via common oxygen atoms, and hosts potassium ions and water molecules. The walls of the $\{Sb_{12}O_{18}\}$ tube consist of $\{Sb_6O_6\}$ rings with a ring width of 2.73 × 2.88 × 2.99 Å ($r(O) = 1.35$ Å). These 6-rings coordinate the potassium ions in a manner similar to crown ethers, with the six distances between the potassium ion and the oxygen atoms ranging from 2.77 to 3.03 Å. In addition, the potassium ions coordinate four water molecules at potassium–oxygen separations of 3.03 to 3.35 Å.

The most conspicuous feature of the SBC-1 structure is, however, the 24-ring tellurium tubular unit hosting the $\{Sb_{12}O_{18}\}$ tubes. The 24-ring has a ring width of 10.99 Å assuming a van der Waals radius $r(Te) = 2.06$ Å. The tellurium unit can be viewed as a tubular sheet or net of tellurium atoms folded around the $\{Sb_{12}O_{18}\}$ tube, where the tellurium tubes are in a hexagonal packing arrangement with the individual tubes connected to its six neighboring tellurium tubes through wall sharing (Figure 1 a). Although unique in its overall structure the tellurium tube is built up from well-known tellurium building blocks, that is, the "dreier chains" found in elementary tellurium, and the Te_2^{2-} dumbbells found in, for example, the two tellurides $BaSbTe_3$ and $BaBiTe_3$.[8] There are also structures known to contain flat nets of Te^- ions, for example, $SrSbTe_3$, and $KBa_2[Ag_3Te_3(Te_3)]$, and further structures that contain T-shaped $TeTe_3^{n-}$ units, for example, $NaTe_3$,[9] and $CsTe_4$.[10]

Each tellurium tube in SBC-1 thus consists of six parallel dreier single chains running along the *c* axis connected to each other through the (001) plane via Te_2^{2-} dumbbells. The tellurium atoms in the dumbbells (Te(1)) are bound to two neighboring Te atoms: one to the other Te(1) atom in the dumbbell (Te(1)–Te(1): 2.78 Å) and the other to an atom denoted Te(2) in the dreier chain (Te(1)–Te(2): 3.18 Å).

---

[*] Dr. A. E. C. Palmqvist
Department of Materials and Surface Chemistry
and Competence Centre for Catalysis
Chalmers University of Technology
412 96 Göteborg (Sweden)
Fax: (+46) 31-160062
E-mail: anders.palmqvist@surfchem.chalmers.se
Dr. B. B. Iversen
Department of Chemistry
University of Aarhus, 8000 Aarhus (Denmark)
Dr. E. Zanghellini
Department of Physics and Engineering Physics
Chalmers University of Technology, 412 96 Göteborg (Sweden)
Dr. M. Behm
Department of Chemical Engineering and Technology
Applied Electrochemistry
Royal Institute of Technology, 100 44 Stockholm (Sweden)
Prof. G. D. Stucky
Department of Chemistry and Biochemistry, Materials Department
University of California, Santa Barbara, CA 93106 (USA)

[**] In reviewing this manuscript, Prof. F. Liebau pointed out that there was no accepted current nomenclature for the new structure presented. This situation has now been addressed and the authors gratefully acknowledge fruitful discussions with Prof. Liebau.[1] Financial support of this work from the Swedish Foundation for International Cooperation in Research and Higher Education (STINT), ONR, Carl Trygger Foundation, and The Swedish Research Council (VR) is greatly appreciated. The authors would like to thank the beam personnel for assistance in the use of beamline X18B at NSLS, which is supported by the U.S. Dept. of Energy, Division of Materials Sciences, under contract No. DE-AC02-98CH10886.

DOI: 10.1002/ange.200351284

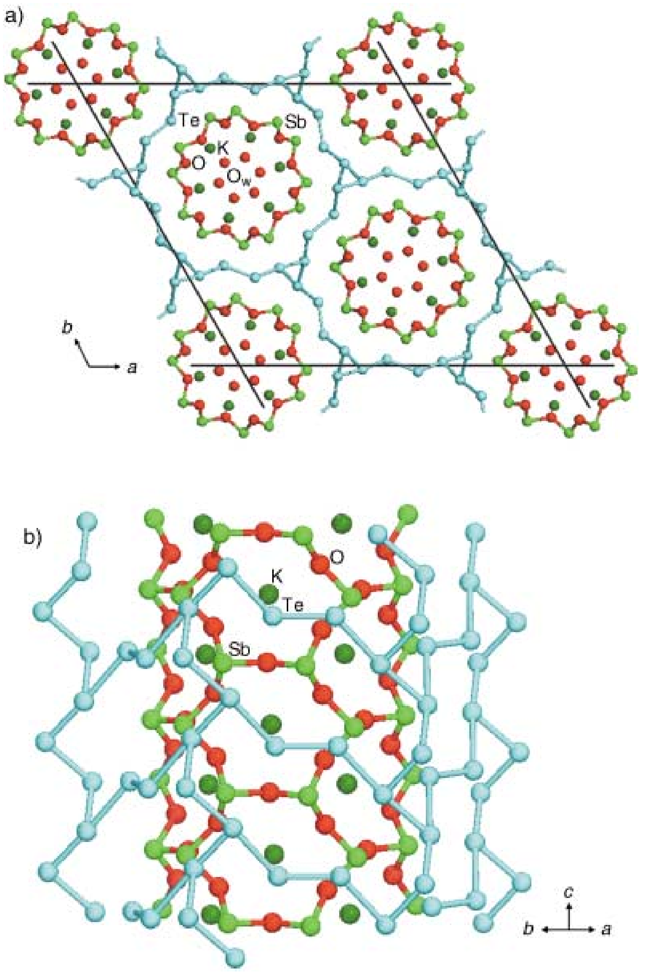

Figure 1. Structure of SBC-1: a) Projection onto the (001) plane showing the 24-ring tubular tellurium unit that hosts the 12-ring $\{Sb_{12}O_{18}\}$ tubular unit, which in turn hosts potassium ions and water molecules (represented by the oxygen O_w); b) a view of one set of tubes with water molecules omitted for clarity.

Interestingly, the Te(1) atoms are located on the opposite side of the $\{Sb_6O_6\}$ rings of the $\{Sb_{12}O_{18}\}$ tube walls from the potassium ions, at a separation of 4.05 Å. However, the Te(1) atom is located away from the center of the 6-ring, with separations between the Te(1) atoms and the six Sb atoms in the ring ranging from 3.40 to 5.51 Å. There are also three Sb atoms located in the neighboring $\{Sb_{12}O_{18}\}$ tube at distances between 3.54 and 4.36 Å from the Te(1) atom. The Te(2) atoms in the dreier chains bond to three tellurium neighbors: two Te(2) atoms within the chain (Te(2)−Te(2): 2.88 Å) besides the one to Te(1) in the Te_2^{2-} dumbbell. These Te−Te distances are comparable to those in elemental tellurium (2.84 Å).[8] The walls of the 24-ring tube consist of six tellurium 12-rings per channel segment (Figure 1b). There are potentially additional weak secondary bonds between Te(1) and Te(2) atoms, which are separated by 3.66 and 4.07 Å. If one considers the shorter distance to be a weak bond, the 12-ring becomes a 10-ring and two 3-rings. Assuming a van der Waals radius $r(\mathrm{Te}) = 2.06$ Å, the ring dimensions are $2.21 \times 2.22 \times 2.71$ Å, which makes the 12-ring non-permeable to H_2O and K^+, and gives a one-dimensional pore system.

Since tellurium and antimony have similar scattering cross sections for X-rays it is difficult to unambiguously distinguish between the two using only X-ray diffraction. For this reason EXAFS analysis of the local structure of antimony was performed to firmly establish the position of these two elements in the structure. Figure 2 shows the experimentally determined local structure of antimony in SBC-1 compared to that of antimony in Sb_2O_3, in the form of the Fourier transform of the EXAFS signal. The local structure of antimony in SBC-1 was found to be similar to that of antimony in Sb_2O_3, and the antimony and tellurium sites in SBC-1 were confirmed as being those shown in Figure 1.

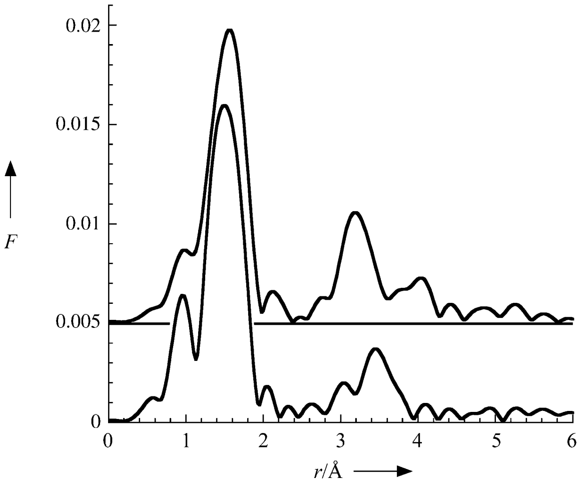

Figure 2. Experimental EXAFS spectra of the Sb K-edge of SBC-1 (bottom) compared to Sb_2O_3 (top) confirming the structure of SBC-1 as presented in Figure 1. F = Fourier transform $F(\chi(k)\,k^2)$; r = radial distance.

To better understand the oxidation state of the host elements in the SBC-1 structure, XANES analyses were performed at the antimony and tellurium K-edges. Figure 3a presents the antimony K-edge XANES spectrum of SBC-1 compared to that of Sb_2O_3. The oxidation state of antimony in SBC-1 is the same as that in Sb_2O_3 (+3), which confirms that the $\{Sb_{12}O_{18}\}$ tubes are charge neutral. Figure 3b shows the experimental and theoretical tellurium K-edge XANES spectrum of SBC-1 compared to the experimentally determined spectrum of TeO_2 and the theoretically calculated spectra of TeO_2 and Sb_2Te_3. It is clear that tellurium in SBC-1 is not oxidized, but instead, on average, is present in a slightly reduced form. Simple electron-counting arguments suggest a mixed tellurium oxidation state with an average of −0.5. Mixed oxidation states of tellurium in polytellurides have been frequently observed, and there are examples where the average tellurium oxidation state is −0.5 and where the structure is an open framework, for example, in $[Cr(en)_3Te_6]$ (en = ethylene diamine).[11] In other examples the oxidation state of tellurium is between 0 and −0.5 and the structure is layered (e.g., Cs_3Te_{22}[12]) or has an open framework (e.g., Cs_4Te_{28}[13]). These polytelluride structures are clathrates according to the suggested nomenclature definitions,[1,14] whereas SBC-1 is a zeoate.

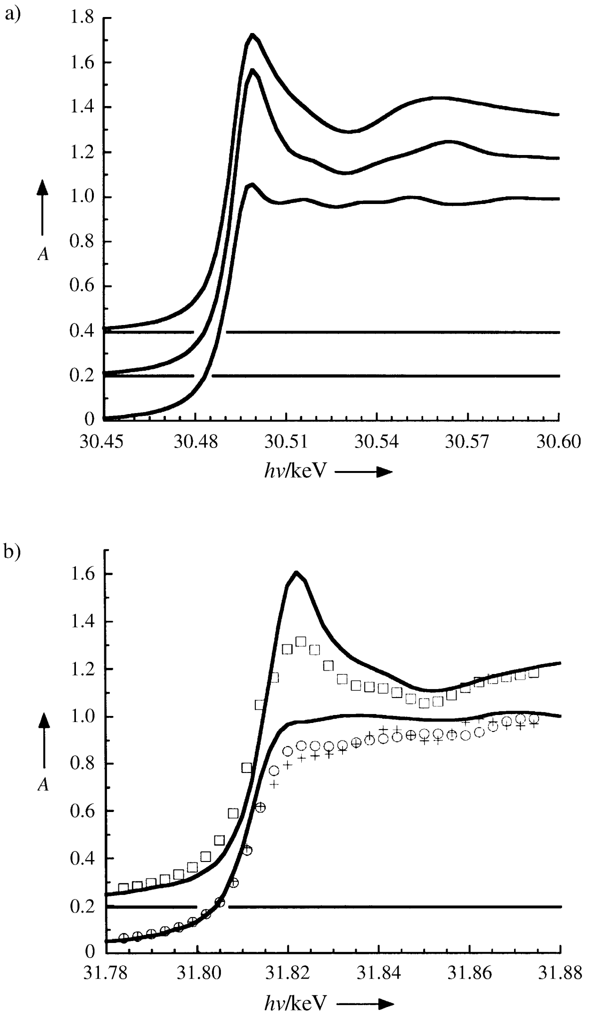

Figure 3. a) Experimental XANES spectra of the Sb K-edge of SBC-1 (top) compared to Sb (bottom) and Sb_2O_3 (middle); b) experimental (solid lines) and theoretical (symbols) XANES spectra of the Te K-edge of SBC-1 (bottom line and ○) compared to Sb_2Te_3 (+) and TeO_2 (top line and □) confirming that the antimony oxide tube is charge neutral and the tellurium is slightly reduced. A = normalized absorption.

SBC-1 can thus be described as a microporous polytelluride with neutral antimony(III) oxide tubular guests, which themselves host potassium ions and water molecules. In our attempt to give the proper crystal chemical formula of SBC-1, following the most recent 2001 IUPAC nomenclature for microporous materials,[15] we were informed that there was no current nomenclature for SBC-1. This situation has now been addressed for the suggested nomenclature of microporous materials of n^{th} order,[1] according to which SBC-1 is a second-order zeoate and its strongly reduced crystal chemical formula is written thus:

$$|(|K_6(H_2O)_6|\,[Sb_{12}O_{18}])_3|\,[Te_{36}]$$

Based on the structural similarities and differences with the cetineite family, SBC-1 was expected to have interesting semiconducting properties. Figure 4 shows the reflectance spectrum of SBC-1 and displays its transparency below

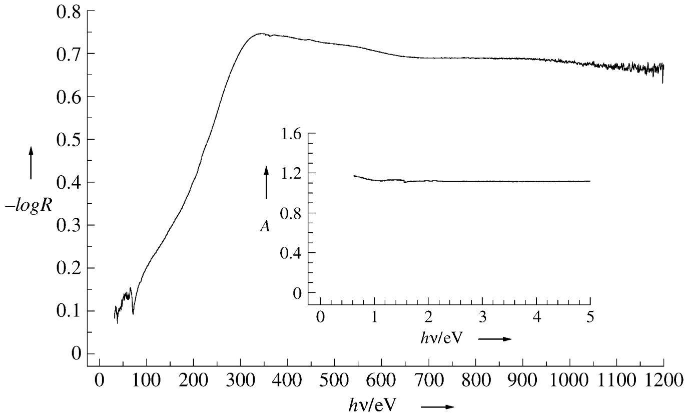

Figure 4. Diffuse reflectance FTIR spectra of a collection of ≈200 single crystals of SBC-1 showing a sharp absorption edge corresponding to an optical bandgap of 0.25 eV. The spectrum represents the logarithm of the inversion of the diffuse reflection from the sample. The inset shows the featureless response in the range 0.8–5 eV. The units on the ordinate axes are arbitrary.

0.25 eV as well as its high absorptivity there above. The inset shows that no other features appear up to at least 5 eV. The transition between these two opposite situations is characterized by a rise of absorptivity that spans about 120 meV. This rise is associated with the Urbach tail below the energy gap and with the energy dependence of the photon absorption coefficient above the gap.

Although the logarithm of the inverse reflection ($-\log R$) is not exactly equivalent to the absorption spectrum, the former is the best estimate of the latter that could be obtained from the available sample with conventional techniques. To estimate the actual energy gap (E_g) from the data, the derivative of the $-\log R$ spectrum with respect to energy was taken. It has been shown that this technique can be applied to estimate the actual value of E_g of both direct- and indirect-bandgap semiconductors directly from the absorption spectrum, within an approximation of about 5 meV.[16] This derivative spectrum presents a single peak centered at about 0.25 eV, with an almost triangular shape and a full-width at half-maximum (FWHM) value of about 120 meV. The presence of a single peak means that SBC-1 is quite probably direct-bandgap semiconductor.

Measurements of the electrical conductivity of SBC-1 were performed on single crystals oriented with a micromanipulator. Figure 5 shows the complex impedance spectra of SBC-1 along its crystallographic c direction and in its (001) plane. The measurements give semicircles, and from their low-frequency minima, the dc resistance R, and the specific conductivity were extracted. SBC-1 was found to have a highly anisotropic conductivity of $5.9\times10^{-3}\,\mathrm{S\,cm^{-1}}$ in the c direction and $2.6\times10^{-6}\,\mathrm{S\,cm^{-1}}$ in the (001) plane.

The value for the c direction is roughly 10^5 times higher than the corresponding values reported for the cetineite family, and since the two structures have the potassium containing $\{Sb_{12}O_{18}\}$ tubular unit in common, we attribute the higher conductivity and narrower bandgap of SBC-1 to its unique tellurium arrangement. The large anisotropy found suggests that conduction takes place in the proximity of the

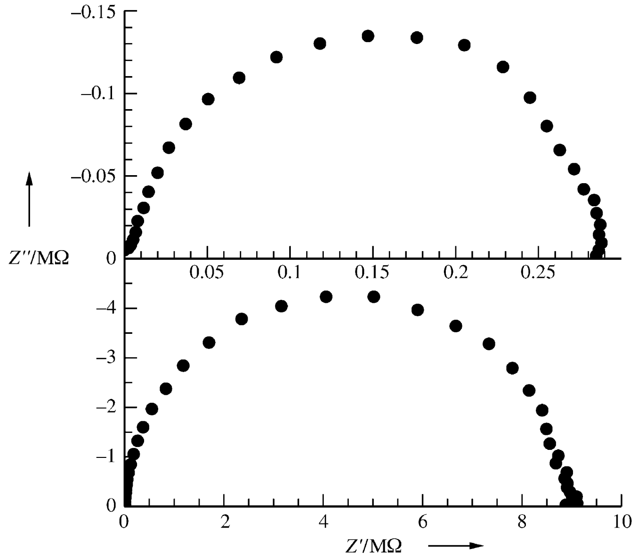

Figure 5. Impedance spectroscopy measurements of the electrical resistance of SBC-1 showing, when recalculated, that the electrical conductivity is highly anisotropic and equal to 2.6×10^{-6} S cm^{-1} in the (001) plane, and 5.9×10^{-3} S cm^{-1} in the *c* direction.

dreier chains rather than the dumbbells of the tellurium tube. The bandgap of SBC-1 is narrower than the 0.33 eV of elementary tellurium, which probably is due to the interaction between the $\{Sb_{12}O_{18}\}$ tubes and the tellurium chains. Clearly the conduction is confined to the *c* direction and thus the SBC-1 structure may be an example of a low-dimensional semiconductor. Band-structure calculations are currently underway to investigate these aspects in more detail.

The SBC-1 structure does not undergo any phase transitions in the temperature range between 100 K and 300 K, and from thermogravimetric and differential thermal analysis it was found to be stable in air up to at least 600 K at atmospheric pressure. At higher temperatures in air SBC-1 appears less stable.

In conclusion, a potentially very useful new material has been prepared by a solvothermal procedure, whose structure was established by a combination of X-ray diffraction and absorption techniques. The material (SBC-1) is a microporous narrow-bandgap semiconductor. It represents a new class of antimony(III) oxide tellurides and is the first example of a second-order zeoate structure.[1] Its narrow bandgap of 0.25 eV, high anisotropy, relatively high conductivity, and microporous structure present possibilities for SBC-1 in new applications, for example, in the fields of chemical sensors, catalysts, membranes, adsorbents, ion exchangers, electro-optics, thermoelectrics, and low-dimensional electronics.

Experimental Section

Crystallization of SBC-1 was effected by solvothermal treatment over 7 days at 453 K in a teflon-lined autoclave using a mixture of Te, Sb, KOH, *n*-propylamine, and water in a molar ratio of 1.00:0.682:1.548:0.68:18.57. The product obtained typically consisted of approximately 40–50 vol % SBC-1, mixed with varying amounts of Sb_2Te_3 and unreacted Te. The synthesis of SBC-1 is sensitive to a number of variables and a more elaborate study concerning this issue is currently underway and will be presented elsewhere.

The crystal structure of SBC-1 was determined at 293 K and 100 K using a Siemens SMART CCD single-crystal X-ray diffractometer ($Mo_{K\alpha}$). Data collection and integration was carried out using the SMART software. Averaging and absorption corrections were done using SADABS. Structure solution and refinement was performed with the SHELX-97 software. SBC-1: trigonal, $R\bar{3}$ (no. 148), $a = b = 27.3361(11)$, $c = 5.6909(3)$ Å at 293 K (27.282(9) and 5.662(2) Å at 100 K), $V = 3682.9(3)$ Å^3, $27\times55\times400$ µm, $\rho_{calcd} = 4.901$ g cm^{-3}, $2\theta_{max} = 56.52°$, $\lambda = 0.7107$ Å, $\mu = 14.05$ mm^{-1}; no. of measured reflections = 7584, no. of unique reflections included in refinement = 1948, least-squares refinement, $N_{par} = 89$, hydrogen atoms were constrained to have $U_{iso} = 1.2\times$ equivalent U_{iso} of the oxygen atom to which they bond, O−H distances were refined with the restraint that they be equal within 0.02 Å, $R(\text{int}) = 0.0329$, $R(\sigma) = 0.0289$, $R1 = 0.0257$ refined against $|F|$, $wR2 = 0.0761$ and GOF = $S = 1.262$ refined against $|F^2|$. Further details on the crystal structure investigations may be obtained from the Fachinformationszentrum Karlsruhe, 76344 Eggenstein-Leopoldshafen, Germany (fax: (+49) 7247-808-666; e-mail: crysdata@fiz-karlsruhe.de), on quoting the depository number CSD-413484.

Tellurium and antimony K-edge XANES and EXAFS measurements were performed at the X18B beamline of NSLS at Brookhaven National Laboratory, New York, on a powdered sample of SBC-1 smeared onto a Scotch tape, which was folded 24 times to ensure the absence of pinholes. Data were treated using the WinXAS 2.1 software.[17] Theoretical calculations of XANES spectra were carried out using the FEFF 8.10 software.[18]

FTIR spectroscopy data were collected in a diffuse reflectance (DR) geometry using a Grasseby Specac unit, model Selector, and a Bruker IFS 66v/S FTIR spectrometer equipped with an MCT detector and a KBr beam-splitter for the MIR, and an InGaAs detector and quartz beam-splitter for the NIR spectral ranges. A set of about 200 hand-picked single crystals was disposed at random on a flat metallic surface. The configuration of the DR unit avoids light reflected from the support surface to reach the detector and the measured radiation comes both from specular reflection at the surfaces of the sample crystals and from diffuse reflectance. The data result from the mean of 100 scans. Special care was taken to ensure that no impurity phases were present during these measurements.

The absorption of SBC-1 in the UV/Vis spectral range was measured in transmission mode through a coarse powder of ground single crystals of SBC-1, placed on a good quality, highly transparent, scotch tape using a Cary 500 UV/Vis/NIR spectrometer.

The electrical conductivity was analyzed on selected single crystals of SBC-1 using impedance spectroscopy in the frequency range of 1 Hz to 10 MHz with a Solartron 1255 HF Frequency Response Analyzer and a Solartron 1296 Dielectric Interface. In the crystallographic *c* direction of SBC-1, impedance measurements were carried out on free-standing freshly cleaved single crystals mounted with a micromanipulator between a sticky copper film and a gold wire. A droplet of silver paste was applied and left to dry between SBC-1 and the gold wire to ensure good electric contact. In the (001) plane the measurements were carried out on single crystals pressed against a gold foil by a gold wire.

Received: February 26, 2003
Revised: November 5, 2003 [Z51284]

Keywords: antimony · microporous materials · semiconductors · tellurium · zeolite analogues

---

[1] F. Liebau, unpublished results; F. Liebau, personal communication.
[2] C. Sabelli, I. Nakai, S. Katsura, *Am. Mineral.* **1988**, *73*, 398–404.

[3] U. Simon, F. Schüth, S. Schunk, X. Wang, F. Liebau, *Angew. Chem.* **1997**, *109*, 1138 – 1140; *Angew. Chem. Int. Ed. Engl.* **1997**, *36*, 1121 – 1124.

[4] F. Starrost, E. E. Krasovskii, W. Schattke, J. Jockel, U. Simon, X. Wang, F. Liebau, *Phys. Rev. Lett.* **1998**, *80*, 3316 – 3319.

[5] X. Wang, F. Liebau, *Eur. J. Solid State Inorg. Chem.* **1998**, *35*, 27 – 37.

[6] A. E. C. Palmqvist, B. B. Iversen, G. D. Stucky, Recent research reports of the 13th International Zeolite Conference (July 8 – 13, Montpellier, France), **2001**.

[7] J. A. Hanko, M. G. Kanatzidis, *Angew. Chem.* **1998**, *110*, 354 – 356; *Angew. Chem. Int. Ed.* **1998**, *37*, 342 – 344.

[8] W. S. Sheldrick, M. Wachhold, *Coord. Chem. Rev.* **1998**, *176*, 211 – 322, and references therein.

[9] P. Böttcher, R. Keller, *Z. Anorg. Allg. Chem.* **1986**, *542*, 144 – 152.

[10] P. Böttcher, U. Kretschmann, *Z. Anorg. Allg. Chem.* **1985**, *523*, 145 – 152.

[11] C. Reisner, W. Tremel, *Chem. Commun.* **1997**, 387 – 388.

[12] W. S. Sheldrick, M. Wachhold, *Angew. Chem.* **1995**, *107*, 490; *Angew. Chem. Int. Ed. Engl.* **1995**, *34*, 450 – 451.

[13] W. S. Sheldrick, M. Wachhold, *Chem. Commun.* **1996**, 607 – 608.

[14] F. Liebau, *Microporous Mesoporous Mater.* **2003**, *58*, 15 – 72.

[15] L. B. McCusker, F. Liebau, G. Engelhardt, *Pure Appl. Chem.* **2001**, *73*, 381 – 394.

[16] W. Z. Shen, *Int. J. Infrared Millimeter Waves* **2002**, *23*, 61 – 69.

[17] T. Ressler, *J. Synchrotron Radiat.* **1998**, *5*, 118 – 122.

[18] A. L. Ankudinov, B. Ravel, J. J. Rehr, S. D. Conradson, *Phys. Rev. B* **1998**, *58*, 7565 – 7576.